Three-Phase AC/AC Motor Drives With Reduced Number of Switches and Without Boost Inductors

E. C. dos Santos Jr., C. B. Jacobina, M. B. de R. Correa, E. R. C. da Silva
Laboratório de Eletrônica Industrial e Acionamento de Máquinas
Departamento de Engenharia Elétrica, Universidade Federal de Campina Grande
Caixa Postal 10105; 58109-970 Campina Grande, PB; Brazil
Fax: +55(83)310-1015; Phone: +55(83)310-1136; Email: jacobina@dee.ufcg.edu.br

Abstract: **This paper presents a three-phase *ac/ac* motor drive with reduced component count. The configurations were conceived to operate with reduced number of switches and without boost inductor. The drives provide both bidirectional power flow and power factor control. The paper presents the analysis and control strategy of the system, including current and PWM voltage controllers. Experimental and simulation results are presented.**

Keywords – **Motor drive, reduced component count, drive boost inductor.**

I. INTRODUCTION

The study of topologies with a reduced number of switches is an important topic in power electronics since it may provide alternative solutions to reduce the cost of energy conversion process while preserving power quality [1–8].

Single-phase to three-phase conversion topologies that do not use a boost inductor were proposed in [7] and also studied in [8] and [9]. Three-phase to three-phase conversion topologies that do not use a boost inductor were proposed in [10]. This paper proposes a drive configuration conceived to operate with reduced number of switches and without boost inductors, but addressed to applications employing a three-phase grid supply two three-phase motors. The three-phase to two three-phase *ac* drive configuration proposed is shown in Fig. 1. This configuration comprises three-phase grid, twelve switches (six-leg), capacitor *dc*-bus, and two three-phase induction machine. The drive provides both bidirectional power flow and power factor control. Besides not using boost inductors, the six-leg configuration uses less switches than the standard double three-phase *ac* drives, that uses nine-leg converter (a six-leg *ac/ac* rectifier/inverter [11] plus a three-leg inverter).

The configurations was conceived for applications where it is necessary to control two machine independently with a significant reduction in the number of components.

II. MACHINE DYNAMIC MODEL

The machines used in this work are three-phase standard machine (machines A and B). Adopting a fixed coordinate reference frame, the mathematical model that describes the dynamic behavior of the three-phase induction machine is given by ($k = a$ for machine A and $k = b$ for machine B):

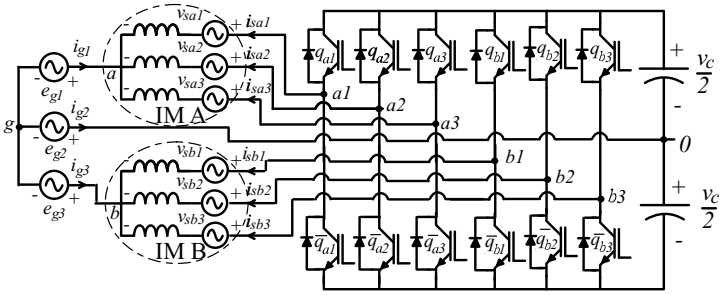

Figura 1 Two three-phase motor drive system with six-leg configuration.

$$\mathbf{v}_{skdq} = r_s\mathbf{i}_{skdq} + \frac{d}{dt}\boldsymbol{\lambda}_{skdq} \quad (1)$$

$$\mathbf{v}_{rkdq} = r_r\mathbf{i}_{rkdq} + \frac{d}{dt}\boldsymbol{\lambda}_{rkdq} - j\omega_{rk}\boldsymbol{\lambda}_{rkdq} \quad (2)$$

$$\boldsymbol{\lambda}_{skdq} = l_s\mathbf{i}_{skdq} + l_{sr}\mathbf{i}_{rkdq} \quad (3)$$

$$\boldsymbol{\lambda}_{rkdq} = l_{sr}\mathbf{i}_{skdq} + l_r\mathbf{i}_{rkdq} \quad (4)$$

$$v_{sko} = r_s i_{sko} + l_{ls}\frac{d}{dt}i_{sko} \quad (5)$$

$$v_{rko} = r_r i_{rko} + l_{lr}\frac{d}{dt}i_{rko} \quad (6)$$

$$T_{ek} = Pl_{sr}(i_{skq}i_{rkd} - i_{skd}i_{rkq}). \quad (7)$$

where $\mathbf{v}_{skdq} = v_{skd} + jv_{skq}$, $\mathbf{i}_{skdq} = i_{skd} + ji_{skq}$, and $\boldsymbol{\lambda}_{skdq} = \lambda_{skd} + j\lambda_{skq}$ are the voltage, current and flux dq vectors of the stator, respectively; v_{sko} and i_{sko} are the homopolar voltage and current of the stator, respectively (the equivalent rotor variables are obtained by replacing the subscript s by r); T_{ek} is the electromagnetic torque; ω_r is the angular frequency of the rotor; r_s and r_r are the stator and rotor resistances; l_s, l_{ls}, l_r and l_{lr} are the self and leakage inductance of the stator and rotor, respectively; l_{sr} is the mutual inductance and P is the number of pair of poles of the machine.

The *dqo* stator variables of the previous model can be determined from the 123 variables by using the transforming equation given by [12]

$$\mathbf{w}_{sk123} = \mathbf{A}_s\mathbf{w}_{skdqo} \quad (8)$$

with $\mathbf{w}_{sk123} = [w_{sk1} \quad w_{sk2} \quad w_{sk3}]^T$, $\mathbf{w}_{skdqo} = [w_{skd}\ w_{skq}\ w_{sko}]^T$ and

$$\mathbf{A}_s = \sqrt{\frac{2}{3}}\begin{bmatrix} 1 & 0 & \frac{\sqrt{2}}{2} \\ -\frac{1}{2} & \frac{\sqrt{3}}{2} & \frac{\sqrt{2}}{2} \\ -\frac{1}{2} & -\frac{\sqrt{3}}{2} & \frac{\sqrt{2}}{2} \end{bmatrix}$$

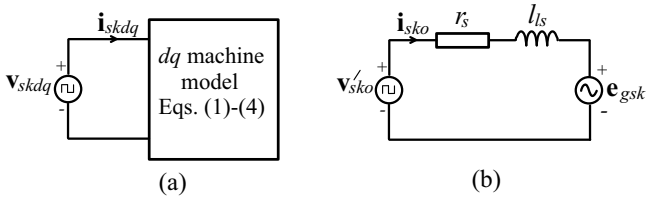

Figura 2 Equivalent circuits for machines A ($k = a$) and B ($k = b$).

Vectors $\mathbf{w}_{sk123}$ and $\mathbf{w}_{skdqo}$ can be voltage or current or flux and $\mathbf{A}_s^{-1} = \mathbf{A}_s^T$.

III. SYSTEM MODEL

The configuration proposed in this paper is shown in Fig. 1. It comprises six-leg (twelve switches), a capacitor *dc*-bus and two three-phase machines. The converter is composed by switches q_{a1}, $\overline{q}_{a1}$, q_{a2}, $\overline{q}_{a2}$, q_{a3}, $\overline{q}_{a3}$, q_{b1}, $\overline{q}_{b1}$, q_{b2}, $\overline{q}_{b2}$, q_{b3} and $\overline{q}_{b3}$. The switch-pairs $q_{a1}-\overline{q}_{a1}$, $q_{a2}-\overline{q}_{a2}$, $q_{a3}-\overline{q}_{a3}$, $q_{b1}-\overline{q}_{b1}$, $q_{b2}-\overline{q}_{b2}$, $q_{b3}-\overline{q}_{b3}$ are complementary. The conduction state of all switches can be represented by an homonymous binary variable q_{a1}, q_{a2}, q_{a3}, q_{b1}, q_{b2}, q_{b3} where $q = 1$ indicates a closed switch while $q = 0$ indicates an open one.

The converter pole voltages are given by

$$v_{a10} = v_{sa1} + e_{g1} + v_{g0} = (2q_{a1} - 1)\frac{E}{2} \quad (9)$$

$$v_{a20} = v_{sa2} + e_{g1} + v_{g0} = (2q_{a2} - 1)\frac{E}{2} \quad (10)$$

$$v_{a30} = v_{sa3} + e_{g1} + v_{g0} = (2q_{a3} - 1)\frac{E}{2} \quad (11)$$

$$v_{b10} = v_{sb1} + e_{g3} + v_{g0} = (2q_{b1} - 1)\frac{E}{2} \quad (12)$$

$$v_{b20} = v_{sb2} + e_{g3} + v_{g0} = (2q_{b2} - 1)\frac{E}{2} \quad (13)$$

$$v_{b30} = v_{sb3} + e_{g3} + v_{g0} = (2q_{b3} - 1)\frac{E}{2} \quad (14)$$

where v_{sai} ($i = 1$ to 3) and v_{sbi} ($i = 1$ to 3) are the machine phase voltages, e_{gj} ($j = 1$ to 3) are the grid voltages, E is the *dc*-bus voltage and v_{g0} is the neutral grid voltage referred to the *dc*-bus mid-point $'0'$ ($v_{g0} = -e_{g2}$).

From (9) to (14), the phase voltages can be obtained as follows

$$v_{sa1} = v_{a10} - e_{g12} \quad (15)$$

$$v_{sa2} = v_{a20} - e_{g12} \quad (16)$$

$$v_{sa3} = v_{a30} - e_{g12} \quad (17)$$

$$v_{sb1} = v_{b10} - e_{g32} \quad (18)$$

$$v_{sb2} = v_{b20} - e_{g32} \quad (19)$$

$$v_{sb3} = v_{b30} - e_{g32} \quad (20)$$

where $e_{g12} = e_{g1} - e_{g2}$ and $e_{g32} = e_{g3} - e_{g2}$.

By using (15)-(20) and (8) it can be written

$$v_{sad} = \sqrt{\frac{2}{3}}(v_{a10} - \frac{1}{2}v_{a20} - \frac{1}{2}v_{a30}) \quad (21)$$

$$v_{saq} = \sqrt{\frac{1}{2}}(v_{a20} - v_{a30}) \quad (22)$$

$$v_{sao} = \frac{1}{\sqrt{3}}(v_{a10} + v_{a20} + v_{a30} - 3e_{g12}) \quad (23)$$

$$v_{sbd} = \sqrt{\frac{2}{3}}(v_{b10} - \frac{1}{2}v_{b20} - \frac{1}{2}v_{b30}) \quad (24)$$

$$v_{sbq} = \sqrt{\frac{1}{2}}(v_{b20} - v_{b30}) \quad (25)$$

$$v_{sbo} = \frac{1}{\sqrt{3}}(v_{b10} + v_{b20} + v_{b30} - 3e_{g32}) \quad (26)$$

Only variables *sao* and *sbo* [see (23) and (26)] depend on e_{g1} to e_{g3}. To make explicit that dependence, new voltage variables *sao*′ and *sbo*′ were introduced, that is, $v'_{sao} = v_{sao} + \sqrt{3}e_{g12}$ and $v'_{sbo} = v_{sbo} + \sqrt{3}e_{g32}$. In this case, the terms depending on the grid voltages are incorporated into the o stator model (5), which become

$$v'_{sao} = r_s i_{sao} + l_{ls}\frac{d}{dt}i_{sao} + e_{gsa} \quad (27)$$

$$v'_{sbo} = r_s i_{sbo} + l_{ls}\frac{d}{dt}i_{sbo} + e_{gsb}. \quad (28)$$

where $e_{gsa} = \sqrt{3}e_{g12}$ and $e_{gsb} = \sqrt{3}e_{g32}$. Substituting (1)-(4), (27) and (28), the model diagram for the dq and o variables can be defined as depicted in Fig. 2. Note that those models are decoupled from each other and o model is coupled with the grid voltages.

The configuration proposed (see Fig. 1) has an unbalanced filter system because of the null impedance in phase 2 of the grid. The *dc*-bus capacitor supply the *ac* power demanded by the unbalance filter.

IV. CONTROL STRATEGY

Decoupling between dq and o variables obtained in the previous sections facilitates controling the system. Nevertheless, the system control strategy still have to be adequately defined to avoid unnecessary coupling of the control loops due to the references definition.

The machine torque control, which includes flux control, can be accomplished by controlling dq currents (e.g., field oriented control) or dq voltages (e.g., volts/hertz control). The grid power factor control is generally achieved by controlling the grid currents, but it can also be carried out directly by controlling the converter input voltage without any current loop.

Initially, consider that torque control for machine A and B as well as power factor control should be done by controlling only the machine phase currents. Assuming that i^*_{sai} ($i = 1$ to 3) are the machine reference phase currents, i^*_{sadqi} ($i = 1$ to 3) are part of the machine phase currents only associated to dq currents (given by (8) with $i^*_{sao} = 0$, i.e., $i^*_{sadq1} = \sqrt{2/3}i^*_{sad}$, $i^*_{sadq2} = -\sqrt{1/6}i^*_{sad} + \sqrt{1/2}i^*_{saq}$ and $i^*_{sadq3} = -\sqrt{1/6}i^*_{sad} - \sqrt{1/2}i^*_{saq}$) defined by

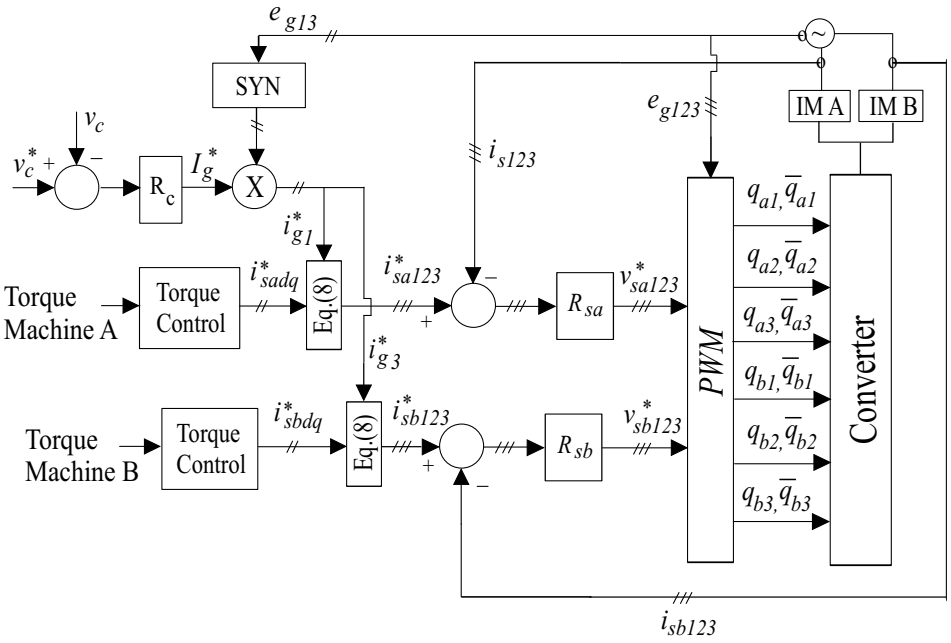

Figura 3 Block diagrams of the system - Phase currents control

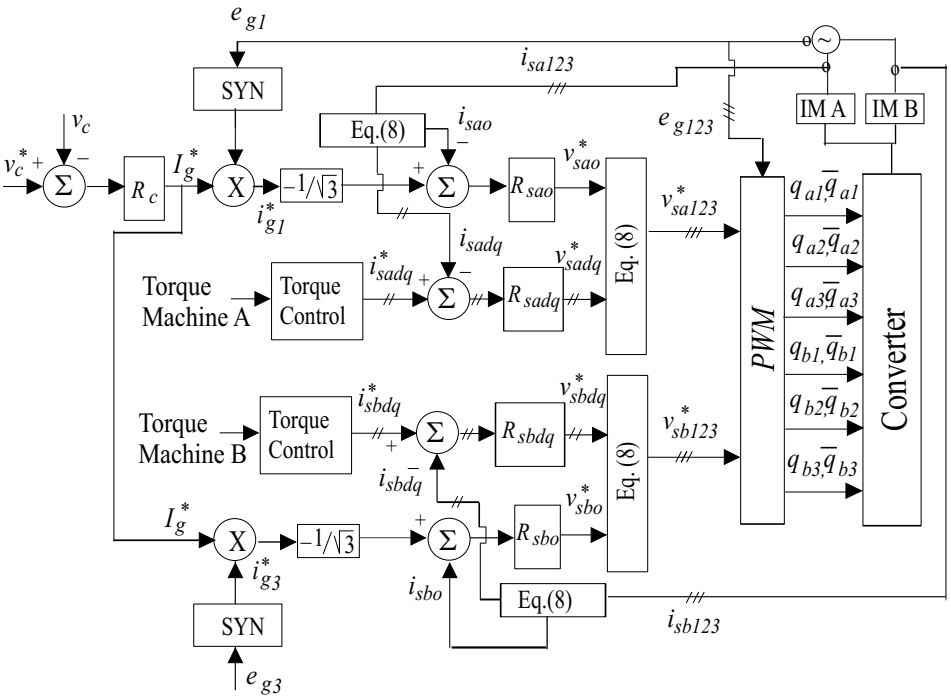

Figura 4 Block diagrams of the system - *dqo* currents control

the torque control and i^*_{sao} are the *sao* reference current (associated to the grid i_{g1} current), the following relation can be defined

$$i^*_{sa1} = i^*_{sadq1} + i^*_{sao} \quad (29)$$
$$i^*_{sa2} = i^*_{sadq2} + i^*_{sao} \quad (30)$$
$$i^*_{sa3} = i^*_{sadq3} + i^*_{sao}. \quad (31)$$

Since $i_{sao} = \frac{1}{\sqrt{3}}(i_{sa1}+i_{sa2}+i_{sa3})$ and $i_{g1} = -i_{sa1}-i_{sa2}-i_{sa3}$, the current i^*_{sao} is given by

$$i^*_{sao} = -\frac{i^*_{g1}}{\sqrt{3}}. \quad (32)$$

Similar relations can be obtained for the machine B where i^*_{g1} is replaced by i^*_{g3}. Then for machine B we have

$$i^*_{sb1} = i^*_{sbdq1} + i^*_{sbo} \quad (33)$$
$$i^*_{sb2} = i^*_{sbdq2} + i^*_{sbo} \quad (34)$$
$$i^*_{sb3} = i^*_{sbdq3} + i^*_{sbo}. \quad (35)$$

Since $i_{sbo} = \frac{1}{\sqrt{3}}(i_{sb1} + i_{sb2} + i_{sb3})$ and $i_{g3} = -i_{sb1} - i_{sb2} - i_{sb3}$, the current i^*_{sao} is given by

$$i^*_{sbo} = -\frac{i^*_{g3}}{\sqrt{3}}. \quad (36)$$

Then i^*_{g1} is controlled by v^*_{sao} and i^*_{g3} is controlled by v^*_{sbo}. The current i^*_{g2} is indirectly controlled, since $i_{g2} = -i_{g1} - i_{g3}$. By using (32), (36) and the previous expression for i^*_{sadq1} to i^*_{sadq3} and i^*_{sbdq1} to i^*_{sbdq3}, (29)-(31) and (33)-(35) become

$$\begin{aligned}
i^*_{sa1} &= \sqrt{2/3} i^*_{sad} - i^*_{g1}/3 && (37)\\
i^*_{sa2} &= -\sqrt{1/6} i^*_{sad} + \sqrt{1/2} i^*_{saq} - i^*_{g1}/3 && (38)\\
i^*_{sa3} &= -\sqrt{1/6} i^*_{sad} - \sqrt{1/2} i^*_{saq} - i^*_{g1}/3 && (39)\\
i^*_{sb1} &= \sqrt{2/3} i^*_{sbd} - i^*_{g3}/3 && (40)\\
i^*_{sb2} &= -\sqrt{1/6} i^*_{sbd} + \sqrt{1/2} i^*_{sbq} - i^*_{g3}/3 && (41)\\
i^*_{sb3} &= -\sqrt{1/6} i^*_{sbd} - \sqrt{1/2} i^*_{sbq} - i^*_{g3}/3. && (42)
\end{aligned}$$

Figs. 3 and 4 shows the control block diagrams for the 123 and *dqo* based control, respectively. The capacitor voltage v_c (*dc*-bus voltage) is adjusted to a reference value by using controller R_c. This controller defines the amplitude I^*_g of all three-phase grid currents. To obtain an unity power factor, instantaneous reference currents i^*_{g1}, i^*_{g2} and i^*_{g3} must be synchronized with the voltages e_{g1}, e_{g2} and e_{g3} (e_{g123}). This is obtained by using block SYN. In Fig. 3, blocks R_{sa} and R_{sb} implement the $i_{sa1} - i_{sa3}$ and $i_{sb1} - i_{sb3}$ currents control, respectively. In Fig. 4, blocks R_{skdq} and R_{sko} implement the *dq* and *o* currents control, respectively, for machine A ($k = a$) and machine B ($k = b$).

When the torque and power factor controls do not use any current loop, the diagram in Fig. 3 and 4 can be directly adapted. In this case, for Fig. 4 the torque controller outputs are the voltages v^*_{sadq} and v^*_{sbdq} (controller R_{sadq} and R_{sbdq} are eliminated).

V. CURRENT CONTROLLER

In this paper the current control is implemented by using a linear discrete control. *dq* currents own only the frequency ω_s, while the *o* currents owns only the frequency ω_g. In order to deal with the filter unbalanced it is more indicated to use a synchronous positive and negative sequence controller (double sequence synchronous controller) [13].

In this paper a double sequence synchronous controller was used. It has the following discrete-time control law

$$\begin{aligned}
x_a(k) &= \cos(\omega_e h)\, x_a(k-1) + \frac{1}{\omega_e}\sin(\omega_e h)\, x_b(k-1)\\
&\quad + 2k_i \frac{1}{\omega_e}\sin(\omega_e h)\, \xi_{sm}(k-1) && (43)\\
x_b(k) &= -\omega_e \sin(\omega_e h)\, x_a(k-1) + \cos(\omega_e h)\, x_b(k-1)\\
&\quad + 2k_i [\cos(\omega_e h) - 1]\, \xi_{sm}(k-1) && (44)\\
v^*_{sm}(k) &= x_a(k) + k_p \xi_{sm}(k) && (45)
\end{aligned}$$

In these equations, h is the sampling period, $\xi_{sm} = i^*_{sm} - i_{sm}$ is the current error ($m = sad$, $m = saq$ and $m = sao$ for the machine A or $m = sbd$, $m = sbq$ and $m = sbo$ for the machine B); x_a and x_b are state-variables of the controller; v^*_{sm} is the reference voltages; ω_e is the current reference frequency ($\omega_e = \omega_s$, i.e., stator frequency, for *dq* controllers or $\omega_e = \omega_g$, i.e., grid frequency, for the *o* controller); and k_p, and k_i are the gains of the controller. This controller gives zero current error in the frequency ω_e.

VI. *PWM* CONTROL

If the desired machine phase voltages are specified by v^*_{sai} and v^*_{sbi} ($i = 1$ to 3), and given the grid voltages e_{g1}, e_{g2} and e_{g3}, then from (9) to (14) the pole voltages can be expressed as

$$\begin{aligned}
v^*_{a10} &= v^*_{sa1} + e_{g12} && (46)\\
v^*_{a20} &= v^*_{sa2} + e_{g12} && (47)\\
v^*_{a30} &= v^*_{sa3} + e_{g12} && (48)\\
v^*_{b10} &= v^*_{sb1} + e_{g32} && (49)\\
v^*_{b20} &= v^*_{sb2} + e_{g32} && (50)\\
v^*_{b30} &= v^*_{sb3} + e_{g32}. && (51)
\end{aligned}$$

Once the pole voltage $v^*_{a10} - v^*_{a30}$ and $v^*_{b10} - v^*_{b30}$ have been determined, we calculate the pulse-widths τ_{a1}, τ_{a2}, τ_{a3}, τ_{b1}, τ_{b2} and τ_{b3} by using

$$\tau_j = \frac{T}{2} + \frac{T}{E} v^*_{j0} \quad \text{for } j = a1 \text{ to } a3 \text{ and } b1 \text{ to } b3 \quad (52)$$

and programmable times or by comparing these voltage (modulating reference signal) to a high frequency triangular carrier signal.

VII. VOLTAGE LIMITS

The voltage limits can be determined by considering that all voltages are purely sinusoidal. Since $v^*_{\max} - v^*_{\min} \leq E$, the *dc*-bus voltage necessary for the configuration shown in Fig. 1 must satisfy both restrictions given by

$$\begin{aligned}
E &\geq l_1 \quad \text{if } (l_1 \geq l_2) \text{ and } (l_1 \geq l_3) && (53)\\
E &\geq l_2 \quad \text{if } (l_2 > l_1) \text{ and } (l_2 \geq l_3) && (54)\\
E &\geq l_3 \quad \text{if } (l_3 > l_1) \text{ and } (l_3 > l_2) && (55)
\end{aligned}$$

where $l_1 = \sqrt{2/3}\,(V_{sadq} + V_{sbdq}) + V_{sao} + V_{sbo} + U_g$, $l_2 = 2\left(\sqrt{2/3} V_{sadq} + V_{sao} + U_g\right)$ and $l_3 = 2\left(\sqrt{2/3} V_{sbdq} + V_{sbo} + U_g\right)$ and U_g denotes the amplitude of the line grid voltage whereas V_{skdq} and V_{sko} represent the amplitude of the machine *dq* voltage and the small amplitude voltage associated to the drop voltage due to the grid current across the *o* impedance, respectively, for machine A ($k = a$) or machine B ($k = b$).

VIII. SIMULATION AND EXPERIMENTAL RESULTS

The systems presented in Fig. 1 have been studied by simulation and experimentally. In both case the switching

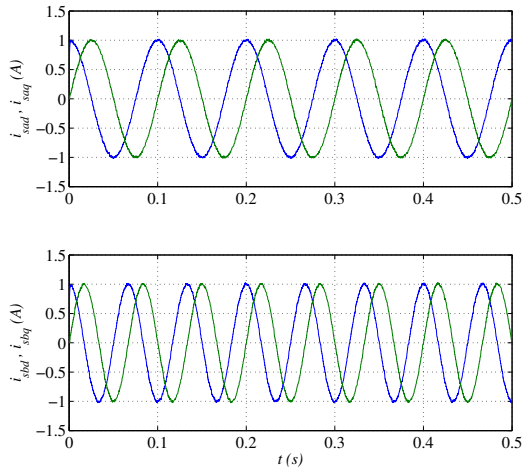

(a)

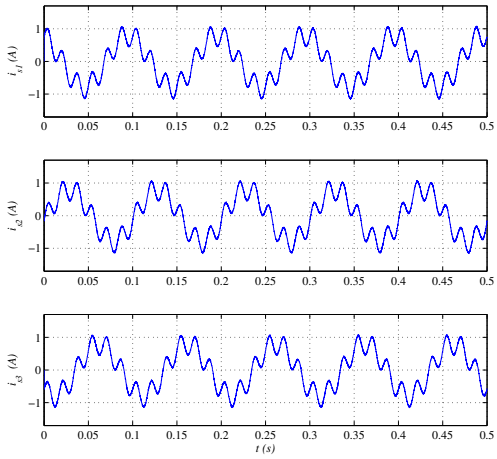

(b)

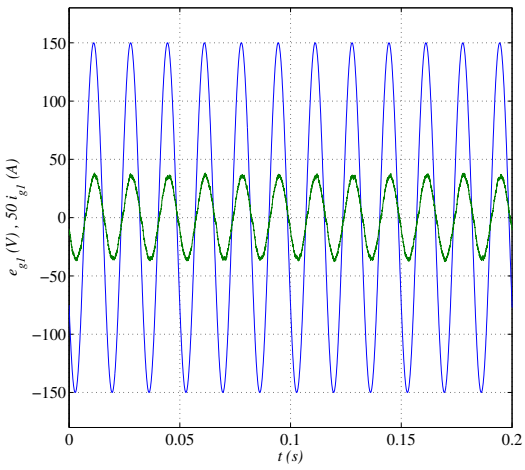

(c)

Figura 5 Simulation results: (a) i_{sad}, i_{saq}, i_{sbd} and i_{sbq}, (b) i_{sa1}, i_{sa2} and i_{sa3}, (c) e_{g1} and 50 i_{g1}

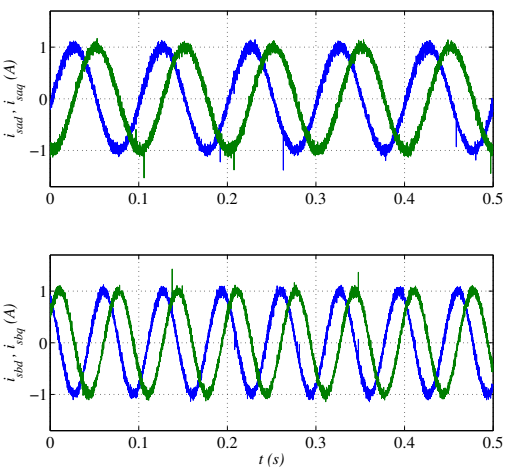

(a)

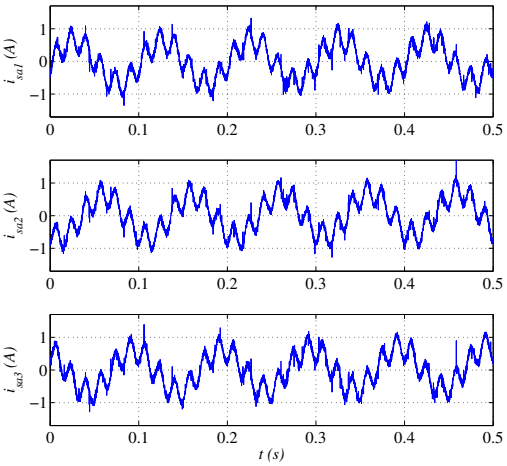

(b)

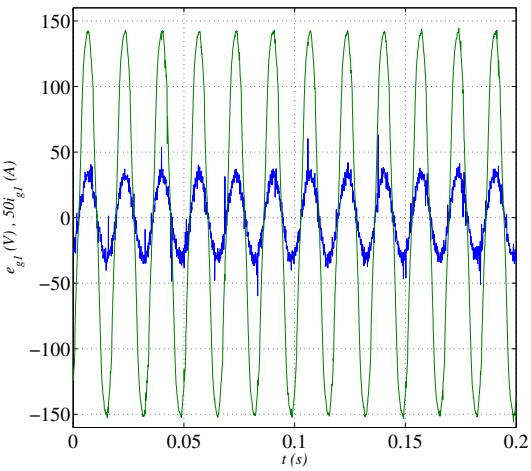

(c)

Figura 6 Experimental results: (a) i_{sad}, i_{saq}, i_{sbd} and i_{sbq}, (b) i_{sa1}, i_{sa2} and i_{sa3}, (c) e_{g1} and 50 i_{g1}

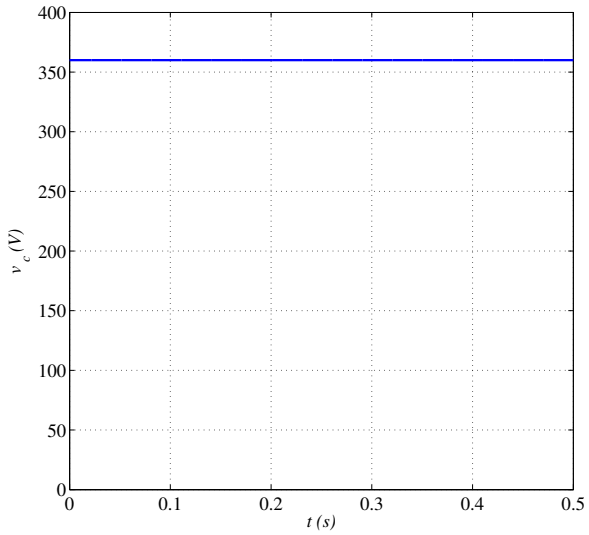

Figura 7 Simulation results: voltage *dc*-bus control.

frequency was $10kHz$ and $C = 1000\mu F$. The set-up used in the experimental tests is based on a microcomputer (PC-Pentium) equipped with appropriate plug-in boards and sensors. This study has shown that the behavior of the systems are adequate. Next some selected results are presented.

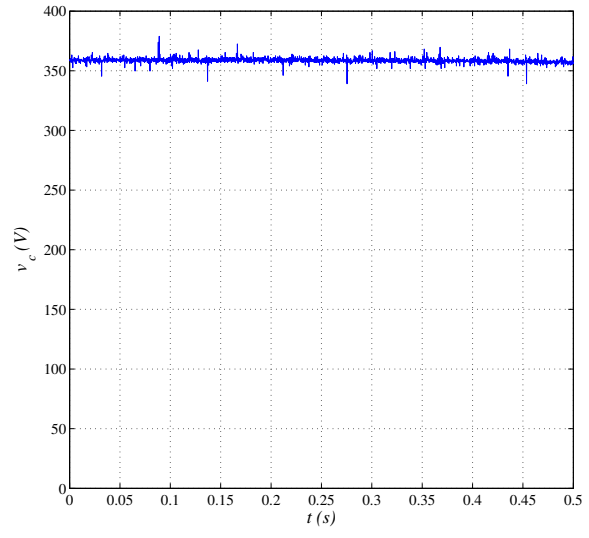

Figura 8 Experimental results: voltage *dc*-bus control.

The results were obtained using current control in the grid (power-factor control) and current control in the machine besides the voltage control of the *dc*-bus.

Fig. 5 (a), (b) and (c) presents simulations results for the machines *dq* currents with 10Hz and 15Hz (of the machine A and B, respectively), phase currents with 10Hz of the machine A and power factor control, respectively.

Fig. 6 (a), (b) and (c) presents experimental results for the machines *dq* currents with 10Hz and 15Hz (of the machine A and B, respectively), phase currents with 10Hz of the machine A and power factor control, respectively.

The capacitor voltage control are shown in Fig. 7 and 8 for the simulated and experimental results. As expected, the machine phase currents present distortions due to the presence of the grid current.

The overall control of the system is effective, even in presence of grid voltage distortions.

IX. CONCLUSIONS

This paper has presented one reduced switch count *ac* drive systems for two three-phase motors. The converters implement both the input rectifier and the inverter without boost inductor filters. The topologies have used no-torque variables to manage the grid current. Their operating principles were presented. Also, it has been shown that their overall performance are adequate. The results have demonstrated the feasibility of the proposed configurations.

REFERENCES

[1] P. Enjeti and A. Rahman, "A new single phase to three phase converter with active input current shaping for low cost ac motor drives," in *Conf. Rec. IAS*, 1990, pp. 935–939.

[2] F. Blaabjerg, S. Freysson, H. H. Hansen, and S. Hansen, "Comparison of a space-vector modulation strategy for a three phase standard and a component minimized voltage source inverter," in *Conf. Rec. EPE*, Sevilha - Spain, 1995, pp. 1806–1813.

[3] M. F. Rahman and L. Zhong, "A current-forced reversible rectifier fed single-phase variable speed induction motor drive," in *Conf. Rec. PESC*, 1996, pp. 114–119.

[4] C.-T. Pan and M.-C. Jiang, "Control and implementation of three phase voltage-double reversible ac to dc converter," in *Conf. Rec. PESC*, 1995, pp. 437–443.

[5] G.-T. Kim and T. A. Lipo, "Vsi-pwm rectifier/inverter system with a reduced switch count," in *Conf. Rec. IAS*, 1995, pp. 2327 – 2332.

[6] C. B. Jacobina, M. B. R. Correa, E. R. C. da Silva, and A. M. N. Lima, "Induction motor drive system for low-power applications," *IEEE Trans. Ind. Applicat.*, vol. 35, no. 5, pp. 52–61, Jan./Feb. 1999.

[7] J. Itoh and K. Fujita, "Novel unity power factor circuits using zero-vector control for single-phase input systems," *IEEE Trans. Power Electron.*, vol. 15, no. 1, pp. 36–43, January 2000.

[8] M. D. Bellar, B. K. Lee, B. Fahimi, and M. Ehsani, "An ac motor drive with power factor control for low cost applications," in *Conf. Rec. APEC*, 2001, pp. 601–607.

[9] E. C. dos Santos Jr, C. B. Jacobina, M. B. R. Corrêa, E. R. C. da Silva, A. C. Oliveira, and E. B. de Sousa Fl., "Control of ac motor drive systems

without boost inductor," in *Proc. of INDUSCON*, 2004.

[10] C. B. Jacobina, E. C. dos Santos Jr, M. B. R. Corrêa, and E. R. C. da Silva, "Ac motor drive with a reduced number of switches and boost inductors," in *Conf. Rec. APEC*, 2005, pp. 601–607.

[11] H. Kohlmeier, O. Niermeyer, and D. F. Scroder, "Highly dynamic four-quadrant ac motor drive with improved power factor and on-line optimized pulse pattern with promc," *IEEE Trans. Ind. Appl.*, vol. 23, no. 6, pp. 1001–1009, Nov./Dec. 1987.

[12] D. C. White and H. H. Woodson, *Electromechanical Energy Conversion*. John Wiley and Sons, 1959.

[13] C. Jacobina, M. Correa, T. Oliveira, A. Lima, and E. da Silva, "Current control of unbalanced electrical systems," in *Conf. Rec. IAS*, 1999, pp. 1011–1017.